

Measurement of the Higgs-boson CP properties using decays into WW and ZZ at the Photon Collider

Photon Collider Physics Working Group (ECFA Study)

P.Nieżurawski, A.F.Żarnecki

Institute of Experimental Physics, Warsaw University,

M.Krawczyk

Institute of Theoretical Physics, Warsaw University

Abstract

Higgs-boson production at the Photon Collider at TESLA is studied for masses from 180 to 350 GeV, using realistic luminosity spectra and detector simulation. Parity of the SM Higgs-boson can be verified from the measurement of the interference effects in the W^+W^- decay channel and of the angular correlations in the decays of W^+W^- and ZZ pairs. SM-like Two Higgs Doublet Model (2HDM II) and model with the generic higgs couplings are considered.

1 Introduction

A photon collider has been proposed as a natural extension of the e^+e^- linear collider project TESLA [1]. The physics potential of a photon collider is very rich and complementary to the physics program of the e^+e^- and hadron-hadron colliders. It is an ideal place to study the mechanism of the electroweak symmetry breaking (EWSB) and the properties of the Higgs-boson. In paper [2] we performed realistic simulation of SM Higgs-boson production at the Photon Collider for W^+W^- and ZZ decay channels, for Higgs-boson masses above 150 GeV. Due to an interference with a large Standard Model background, the process $\gamma\gamma \rightarrow higgs \rightarrow W^+W^-/ZZ$ turns out to be sensitive not only to the Higgs-boson partial width to $\gamma\gamma$, $\Gamma_{\gamma\gamma}$, but also to the phase of the $\gamma\gamma \rightarrow h$ coupling, $\phi_{\gamma\gamma}$. A precise measurement of both $\Gamma_{\gamma\gamma}$ and $\phi_{\gamma\gamma}$ seems to be crucial for determination of the Higgs-boson couplings, see also [3, 4, 5, 6, 7]. In [2] we have found that this is extremely important to combine both W^+W^- and ZZ channels, as the first one due to a large background is very sensitive to a phase, while the second - to a partial width. From combined analysis of W^+W^- and ZZ decay channels the $\gamma\gamma$ partial width can be measured with an accuracy of 3 to 8% and the phase of the amplitude with an accuracy between 30 and 100 mrad.

In this paper we extend this analysis by considering in detail various extensions of the Standard Model, in particular the SM-like Two Higgs Doublet Model 2HDM II with and without CP-conservation. We perform the combined analysis of W^+W^- and ZZ invariant-mass distributions and extract the corresponding Higgs-boson couplings ($\tan\beta$). For 2HDM model with a CP violation, we estimate precision of the $H - A$ mixing angle.

We also consider here a potential of establishing CP-properties of Higgs-bosons in a general CP-violating model from a combined analysis of the angular distributions of the W^+W^- and ZZ decay-products. In this approach a CP properties of the Higgs boson can be studied independently on a production mechanism. We consider a model with generic, CP-violating higgs couplings to vector bosons, leading to different angular distributions for a scalar- and pseudoscalar-type of couplings. From such measurement the CP-parity of the observed Higgs state can be determined. Precision in the determination of couplings can be significantly improved if measurement of angular distributions is combined with the invariant-mass one. However, in such case additional model assumptions are needed.

2 Measurement of the $h(H) \rightarrow \gamma\gamma$ width and phase from the invariant-mass distributions

The Compton back-scattering of a laser light off high-energy electron beams is considered as a source of high energy, highly polarized photon beams [8]. According to the current design [1], the energy of the laser photons is assumed to be fixed for all considered electron-beam energies. With 100% circular polarization of laser photons and 85% longitudinal polarization of the electron beam the luminosity spectra peaked at high $\gamma\gamma$ invariant masses is expected.

The analysis bases on the CompAZ parametrization [9] of the realistic luminosity spectra for a Photon Collider at TESLA [10]. We assume that the centre-of-mass energy of colliding electron beams $\sqrt{s_{ee}}$, is always optimised for the production of a Higgs boson with a given mass. The event generation according to the cross-section formula for a vector-boson production including the higgs contribution [3, 4, 11] is done with PYTHIA 6.152 [12]. The fast simulation program SIMDET version 3.01 [13] is used to model the TESLA detector performance. The selection cuts are applied to select $W^+W^- \rightarrow q\bar{q}q\bar{q}$ and $ZZ \rightarrow l\bar{l}q\bar{q}$ events ($l = \mu, e$).

All results presented in this paper were obtained for an integrated luminosity corresponding to one year of the photon collider running, as given by [10]. The total photon-photon luminosity increases from about 600 fb^{-1} for $\sqrt{s_{ee}} = 305 \text{ GeV}$ (optimal beam energy choice for $M = 200 \text{ GeV}$) to about 1000 fb^{-1} for $\sqrt{s_{ee}} = 500 \text{ GeV}$ (optimal beam energy choice for $M = 350 \text{ GeV}$).

2.1 Standard Model analysis

In this section we summarise results of [2], where the feasibility of measuring Standard Model Higgs-boson production in W^+W^- and ZZ decay channels in $\gamma\gamma$ option of TESLA has been studied for a Higgs-boson mass above 150 GeV . We have studied the signal, i.e. the Higgs-boson decays into the vector bosons, and the background from direct vector-bosons production. For the ZZ final-state a direct, i.e. non-resonant $\gamma\gamma \rightarrow ZZ$ process, is rare as it occurs via loop only. On contrary, the non-resonant W^+W^- production is a tree-level process, and is expected to be large. Therefore, also an interference between the signal of W^+W^- production via the Higgs resonance and the background from direct production may be large. This effect can be used to access an information about the phase of the $higgs \rightarrow \gamma\gamma$ coupling, $\phi_{\gamma\gamma}$. For the Higgs-boson masses around 350 GeV we found that the amplitude phase $\phi_{\gamma\gamma}$ is more sensitive to the loop contributions of new, heavy charged particles than the $\Gamma_{\gamma\gamma}$ itself.

The invariant-mass resolution obtained from a full simulation of W^+W^- and ZZ events based on the PYTHIA and SIMDET programs, has been parametrized as a function of the $\gamma\gamma$ centre-of-mass energy, $W_{\gamma\gamma}$. The distributions of the reconstructed invariant mass for $\gamma\gamma \rightarrow W^+W^-$ and $\gamma\gamma \rightarrow ZZ$ events are shown in Figs. 1, upper and lower panels, respectively. Results from a full event simulation based on PYTHIA and SIMDET are compared with the distribution obtained from the numerical convolution of the relevant cross-sections with the CompAZ spectra and the parametrized detector resolution.

Based on a parametric description of the expected mass distributions, many experiments were simulated, each corresponding to one year of a Photon Collider running at TESLA at a nominal luminosity. The “theoretical” distributions were then fitted, simultaneously to the observed W^+W^- and ZZ mass spectra, with the width $\Gamma_{\gamma\gamma}$ and phase $\phi_{\gamma\gamma}$ considered as the only free parameters. Results of the fits performed for different Higgs-boson masses and at different electron-beam energies are shown in Figs. 2. They indicate that with a proper choice of the electron-beam energy, the $\gamma\gamma$ partial width can be measured with an accuracy of 3 to 8%, while the phase of the amplitude with an accuracy between 35 and 100 mrad, see Fig. 2. The $\phi_{\gamma\gamma}$

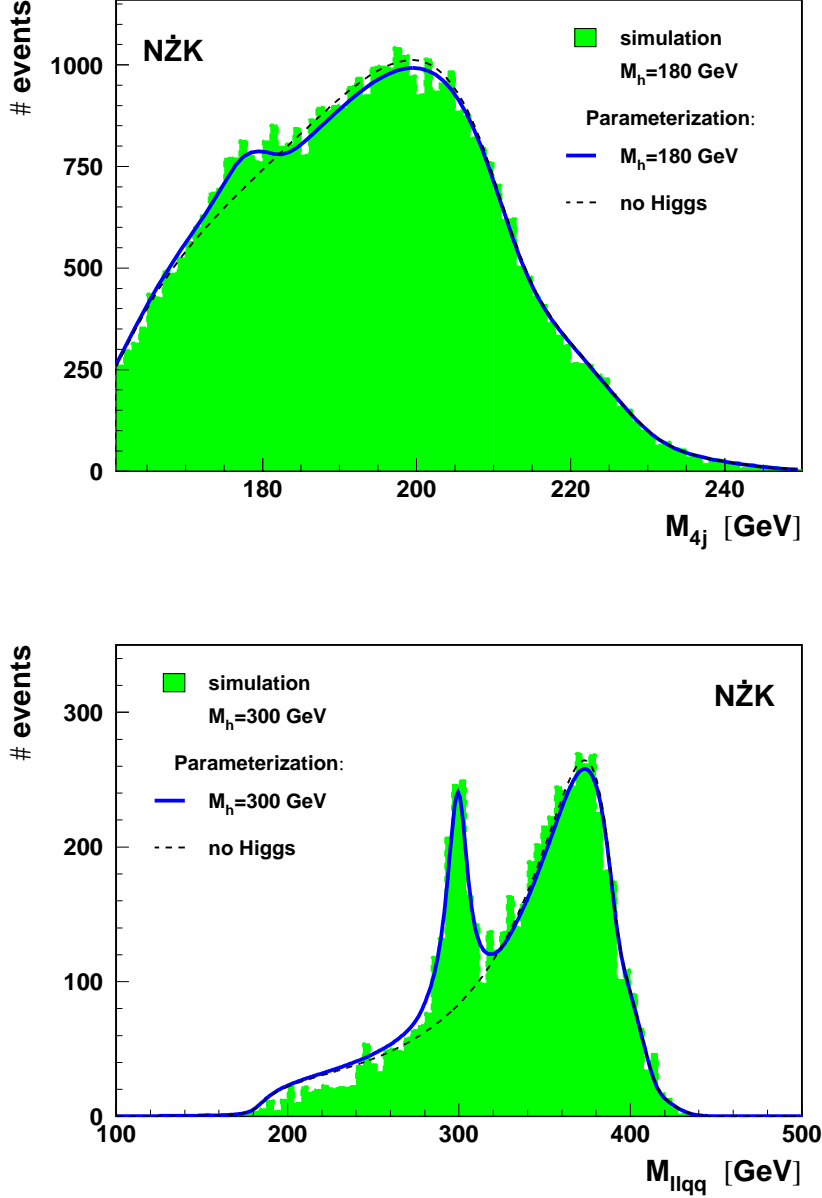


Figure 1: Distribution of the reconstructed invariant mass for $\gamma\gamma \rightarrow W^+W^-$ events with a SM Higgs-boson mass of 180 GeV and an electron-beam energy of 152.5 GeV (upper plot) and for $\gamma\gamma \rightarrow ZZ$ events, with a SM Higgs-boson mass of 300 GeV and an electron-beam energy of 250 GeV (lower plot). Results from the simulation based on PYTHIA and on the SIMDET detector-simulation (histogram) are compared with the distribution obtained by the numerical convolution of the cross-section formula with the CompAZ energy-spectra for photon-beams and parametrization of the detector resolution (solid line). The distribution expected without the higgs contribution is also shown (dashed line) [2].

measurement opens a new window to a precise determination of the Higgs-boson couplings and to search of a “new physics”. It turns out that the phase is constrained predominantly by the W^+W^- invariant-mass distribution, thanks to large interference effects between Higgs-boson decay and nonresonant W^+W^- production. However, two-photon width of the Higgs-boson is much better constrained by the measurement of the ZZ mass spectra, as the nonresonant background is much smaller here. A precise determination of both parameters is only possible when both measurements are combined.

2.2 Determination of the Higgs-boson couplings in the SM-like Two Higgs Doublet Model

In our previous analysis [2] we have considered possible deviations from the Standard Model predictions resulting from the loop contributions to the $h\gamma\gamma$ vertex of new heavy charged particles. However, deviations in the two-photon width and phase can also appear if the couplings of the Higgs-boson to the other particles are different than those predicted by the Standard Model. This possibility is studied in this paper, see also [14].

As the simplest model with non-standard higgs couplings we consider Standard Model-like Two Higgs Doublet Model (2HDM II) [14]. We study a simple version of the so called solution B, where the lightest Higgs-boson h couplings to fermions are fixed and they have the same values as in the Standard Model, except that for up-type fermions the sign is opposite. The couplings of h to the EW gauge-bosons may differ from the corresponding SM predictions. There is only one parameter in such model, β , and all remaining couplings of h and all couplings of H and A can be expressed in terms of it, as presented in the table 1.¹

One expects significant deviations from the Standard Model predictions for a light Higgs-boson h , both for the two-photon width and phase, for $\tan\beta \ll 1$. As compared to the SM there is a change of a relative sign of the top-quark and the W contribution, therefore the two-photon width in 2HDM II (B) is significantly larger than in the Standard Model, where these two contributions partly cancel each other. For $\tan\beta \sim 1$ the two-photon width decreases,

¹ h and H couplings to the charged higgs boson H^\pm are calculated according to the 2HDM II potential [14] assuming $\mu=0$.

	h	H	A
χ_u	-1	$-\frac{1}{\tan\beta}$	$-i \gamma_5 \frac{1}{\tan\beta}$
χ_d	$+1$	$-\tan\beta$	$-i \gamma_5 \tan\beta$
χ_V	$\cos(2\beta)$	$-\sin(2\beta)$	0

Table 1: Couplings of the neutral Higgs-bosons to fermions and vector bosons, relative to the Standard Model couplings, for the considered solution B of the SM-like Two Higgs Doublet Model (2HDM II).

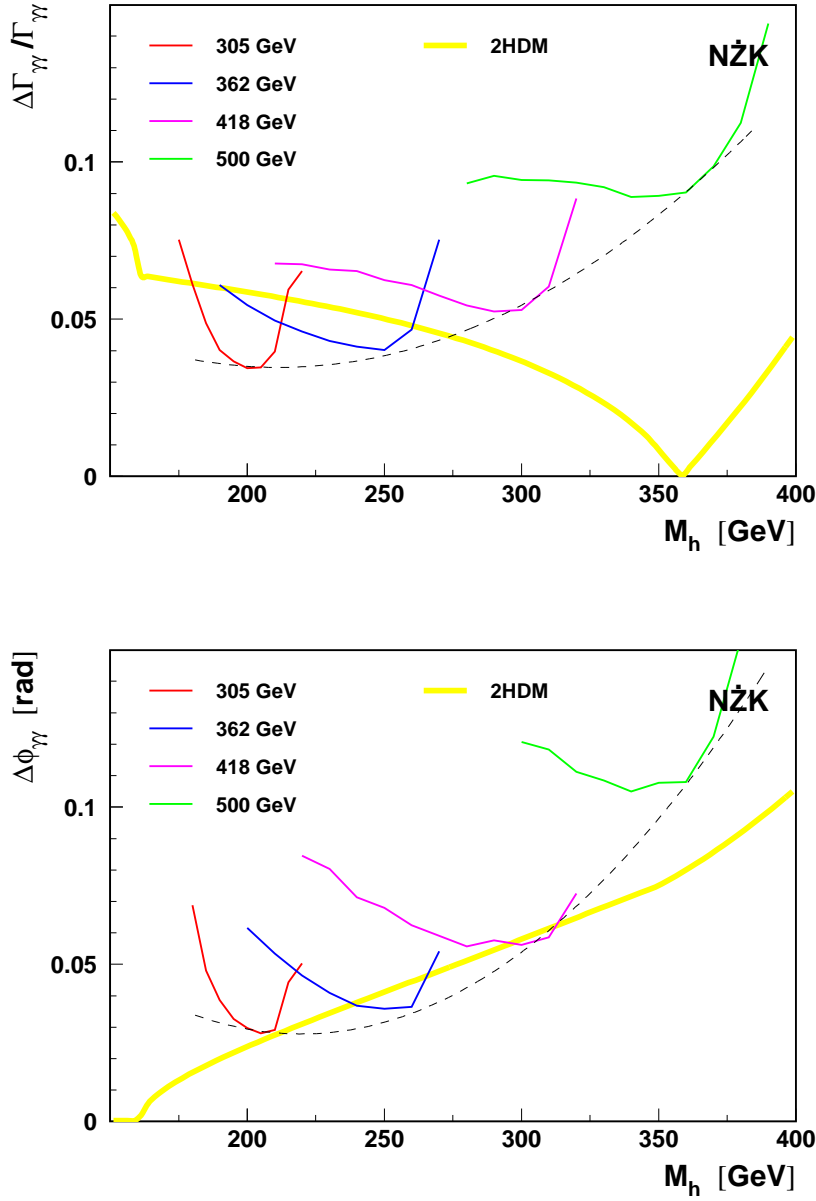


Figure 2: Statistical error in the determination of the Higgs-boson width $\Gamma_{\gamma\gamma}$ (upper plot) and phase $\phi_{\gamma\gamma}$ (lower plot), from the combined fit to the observed W^+W^- and ZZ mass spectra, as a function of the Higgs-boson mass M_h . Results are given for four various centre-of-mass energies of colliding electron beams $\sqrt{s_{ee}}$, as indicated in the plot. The yellow (tick) line shows the size of the deviations expected in the SM-like 2HDM II [14] with an additional contribution due to the charged Higgs-boson of mass $M_{H^+} = 800$ GeV. The thin dashed line is included to guide the eye. [2]

due to the suppressed W -loop contribution ($g_{hWW} \sim 0$). Finally, for large values of $\tan\beta$ ($\cos(2\beta) \approx -1$) the two-photon width of the light Higgs-boson h tend to be very close to the expectations of the Standard Model. The only difference is due to the presence of the charged Higgs-boson in the loop. The difference resulting from the opposite, as compared to SM, sign of the down-type fermion contributions is very small and can be neglected.

Results for the light Higgs-boson h with mass $M_h = 300$ GeV, from the measurement of the two-photon width (times the vector-boson branching ratio) and phase are presented in Fig. 3 for various $\tan\beta$ values. Error contours (1σ) on the expected deviation from the Standard-Model predictions correspond to one year of photon collider running, i.e. $L_{\gamma\gamma} \approx 840 \text{ fb}^{-1}$. In the combined fit to the invariant-mass distributions for W^+W^- and ZZ events we take the advantage of the fact that the ratio of the corresponding branching ratios $BR(h \rightarrow ZZ)/BR(h \rightarrow W^+W^-)$ is expected to be the same as in the Standard Model. Charged Higgs-boson mass is set to 800 GeV. Results presented in Fig. 3 show that the measurement of the two-photon width and phase for the light Higgs-boson h decaying into W^+W^- and ZZ would allow a precise determination of the $\tan\beta$ value. The possible ambiguity in the measurement of the two-photon width is resolved by the phase measurement, which clearly distinguishes between low $\tan\beta$ and large $\tan\beta$ solutions. The statistical error on the extracted $\tan\beta$ value is shown in Fig. 4 for different values of light Higgs-boson mass M_h .

For all considered Higgs-boson masses the expected error in the $\tan\beta$ determination is smallest for $\tan\beta$ close to 1. This is because the Higgs-boson coupling to the vector bosons is most sensitive to $\tan\beta$, for such values. The precision of $\tan\beta$ measurement, for $\tan\beta \sim 1$, deteriorates with an increase of the Higgs-boson mass. It changes from about 1% for mass of 200 GeV to about 10% for mass of 350 GeV. For very high and very low $\tan\beta$, when the relative Higgs-boson coupling to vector bosons is close to ± 1 (table 1), precise measurement of $\tan\beta$ is not possible.

The measurement of the two-photon width and phase has been investigated also for the heavy scalar Higgs-boson H of the SM-like Two Higgs Doublet Model (solution B), with couplings as given in table 1. In this case we consider only $0.2 \leq \tan\beta \leq 1$, since for $\tan\beta > 1$ both the top-quark and W contributions are strongly suppressed and the precision of the measurement deteriorates fast. For $\tan\beta \sim 1$ both the two-photon width and phase of the heavy scalar Higgs-boson H are close to the expectations of the Standard Model (for a given M_H). For decreasing values of $\tan\beta$ the W -loop contribution decreases, while the top-quark one increases and as a result, the two-photon width decreases slightly for $\tan\beta \sim 0.5$ and then starts to increase with $\tan\beta$. Finally, for $\tan\beta \sim 0.1$ the Higgs-boson decays to $c\bar{c}$ start to dominate. The expected number of events with the W^+W^- and ZZ decays drops rapidly and the measurement becomes problematic again.

The results of the analysis of the measurement of the two-photon width and phase, for the heavy scalar H with mass $M_h = 300$ GeV, are presented in Fig. 5. Light Higgs-boson mass is set to 120 GeV and that of the charged Higgs-boson to 800 GeV.

Error contours (1σ) on the measured deviation from the Standard Model predictions are presented. Results show that a precise determination of $\tan\beta$, in the considered region of

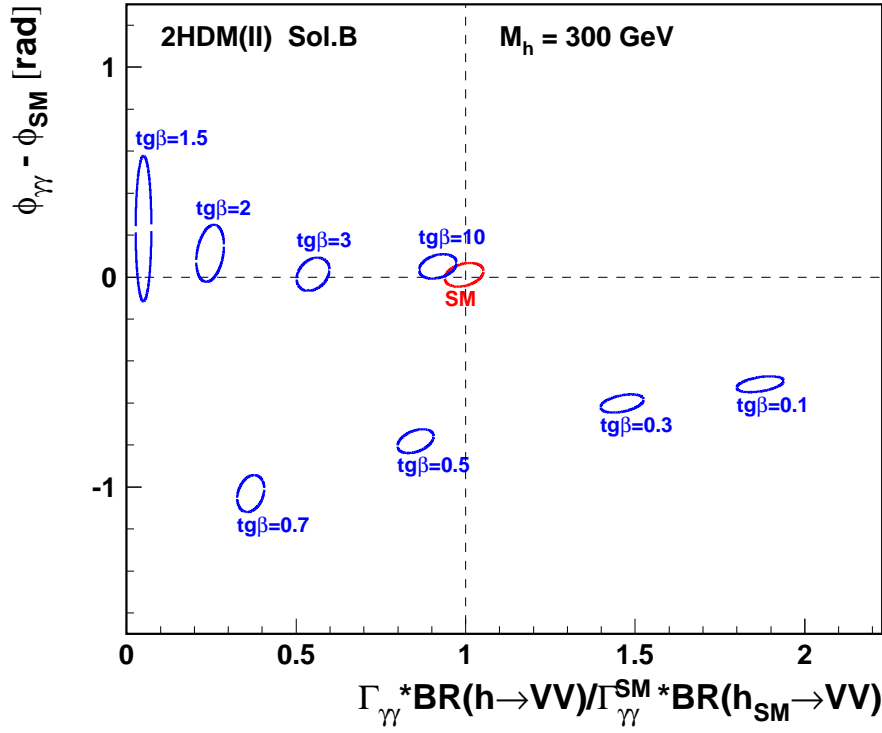


Figure 3: The deviation from the SM of for the light Higgs-boson h with mass $M_h = 300$ GeV in the SM-like 2HDM II (B), with charged Higgs-boson mass of 800 GeV for different values of $\tan\beta$. Error contours (1σ) on the measured deviation from the Standard Model predictions for the $h \rightarrow \gamma\gamma$ phase $\phi_{\gamma\gamma}$ and for the decay width $\Gamma_{\gamma\gamma}$ times vector boson branching ratio $BR(h \rightarrow VV)$, correspond to $L_{\gamma\gamma} \approx 840 \text{ fb}^{-1}$. Red contour labelled 'SM' indicates the expected precision for the Standard Model.

parameters, should also be possible for heavy scalar H decaying to W^+W^- and ZZ .

Shown in Fig. 6 is the statistical error on the extracted $\tan\beta$ values. Results are given for four values of heavy scalar Higgs-boson mass M_H , from 200 to 350 GeV. The expected error in the $\tan\beta$ determination is small (1–3 %) for low $\tan\beta$, $\tan\beta \approx 0.25$. For larger values of $\tan\beta$, the precision depends strongly on the Higgs-boson mass. For mass of 200 GeV it changes between 3 and 8 %, whereas for mass of 350 GeV it is between 3 and 20 %.

2.3 Determination of CP properties of the Higgs boson in the SM-like Two Higgs Doublet Model

In the general Two Higgs Doublet Model [15], the mass eigenstates of the neutral Higgs-bosons h_1 , h_2 and h_3 do not match CP eigenstates h , H and A . We consider here a SM-like version of the CP-violating Two Higgs Doublet Model, with CP violation through a small mixing between

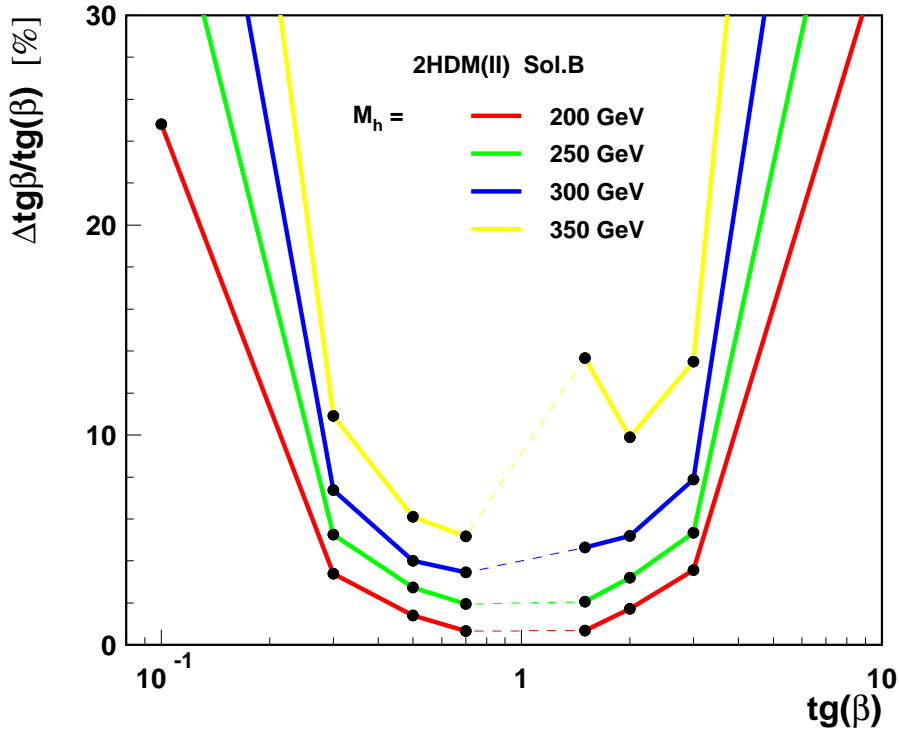


Figure 4: Statistical error in the determination of $\tan\beta$, for four values of light Higgs-boson mass M_h . The simultaneous fit to the observed W^+W^- and ZZ mass spectra, is considered for the SM-like 2HDM II (B), with charged Higgs-boson mass of 800 GeV. Centre-of-mass energy of colliding electron beams $\sqrt{s_{ee}}$ is optimised for each mass M_h .

H and A states. We consider a simple version of such model, where the couplings of the lightest higgs mass-eigenstate h_1 (with mass 120 GeV) are expected to correspond to the couplings of h boson, whereas couplings of h_2 and h_3 states can be described as the superposition of H and A couplings (see table 1), as follows:

$$\begin{aligned}\chi_X^{h_1} &\approx \chi_X^h \\ \chi_X^{h_2} &\approx \chi_X^H \cdot \cos \Phi_{HA} + \chi_X^A \cdot \sin \Phi_{HA} \\ \chi_X^{h_3} &\approx \chi_X^A \cdot \cos \Phi_{HA} - \chi_X^H \cdot \sin \Phi_{HA}\end{aligned}\tag{1}$$

where X denotes a fermion or a vector boson, $X = u, d, V = W$ or Z . We study the feasibility of the mixing angle Φ_{HA} determination from the combined measurement of the two-photon width and phase for the higgs mass-eigenstate h_2 . We consider only small CP-violation effects, i.e. $|\Phi_{HA}| \ll 1$.

Results of the combined analysis (WW/ZZ decay channels) of the measurement of the two-photon width (times vector-boson branching ratio) and phase for the scalar Higgs-boson h_2 with mass $M_{h_2} = 300$ GeV, are presented in Fig. 7. A light Higgs-boson has mass $M_{h_1} = 120$ GeV while $M_{H^\pm} = 800$ GeV. The simultaneous fit to the observed W^+W^- and ZZ mass-spectra was

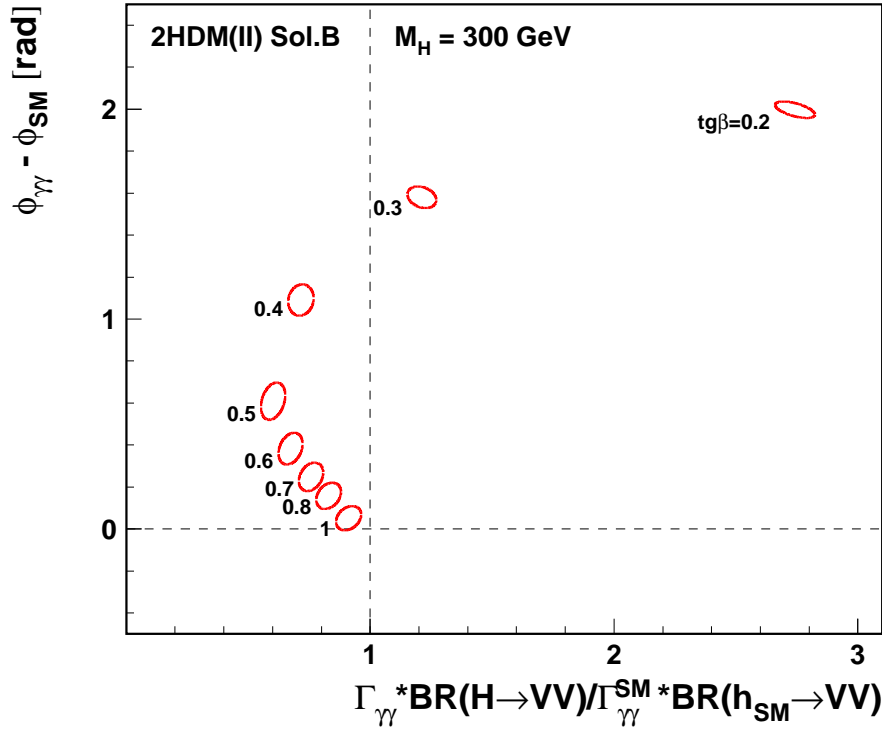


Figure 5: As in Fig. 3 for the heavy Higgs-boson H with mass 300 GeV. A light Higgs-boson mass is assumed to be $M_h = 120$ GeV.

performed. Error contours (1σ) on the measured deviation from the Standard Model predictions are shown for $\Phi_{HA} = 0$, i.e. when CP is conserved, and for CP violation with $\Phi_{HA} = \pm 0.3$. Even a small CP-violation can significantly influence the measured two-photon width and two-photon phase, and therefore it is possible to determine precisely both the CP-violating mixing angle Φ_{HA} and $\tan\beta$.

Next, we address a question: how well one can establish the fact that in a model CP is conserved? The answer can be read out from Fig. 8 where the statistical error in the determination of the $H - A$ mixing angle Φ_{HA} , around $\Phi_{HA} = 0$ value, is shown. The results are presented as a function of $\tan\beta$ for four values of Higgs-boson mass M_{h_2} , from 200 to 350 GeV. As above, we assume a light Higgs-boson mass $M_{h_1} = M_h = 120$ GeV, charged Higgs-boson mass of 800 GeV.

For low value of $\tan\beta$, $\tan\beta \approx 0.25$, the expected error is of the order of 20–25 mrad and does not depend on the heavy Higgs-boson mass. For larger values of $\tan\beta$ the precision worsens for small Higgs-boson masses. For $\tan\beta = 1$ the expected error changes from 35 mrad for mass of 350 GeV to about 90 mrad for mass of 200 GeV.

To summarize this part, in the 2HDM model the Higgs-boson couplings to the vector bosons are always as for a scalar (say in the SM) with a modification by some functions, i.e. they are

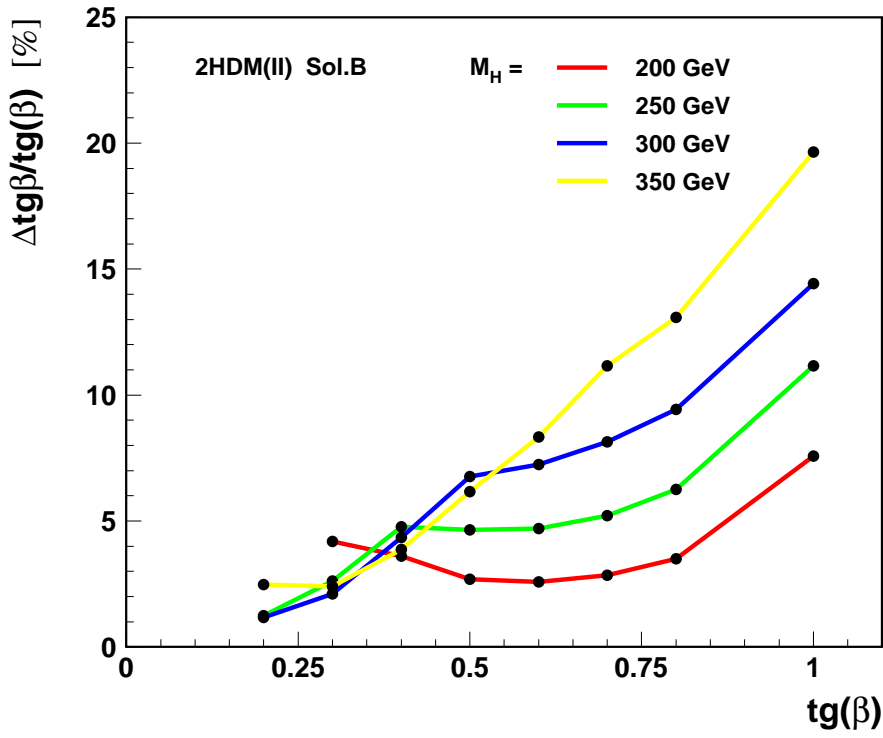


Figure 6: As in Fig. 4 for a heavy Higgs boson H , with a light Higgs-boson mass of $M_h = 120$ GeV.

proportional to g_h^{SM} . This is because there is no pseudoscalar coupling to W^+W^- and ZZ in this model ($\chi_V^A \equiv 0$). The measured W^+W^- and ZZ mass-spectra are sensitive to the CP-violating $H - A$ mixing angle only via a Yukawa coupling, more precisely due of the top-quark loop contribution to the $h_2\gamma\gamma$ vertex. In the next section we will consider more general case, with a generic pseudoscalar couplings to the gauge bosons.

3 Secondary decay analysis for generic model with CP violation.

In the general case, with a generic pseudoscalar coupling of Higgs-boson to vector bosons, not only the invariant-mass distribution of the reconstructed W^+W^- and ZZ events, as discussed in sec. 2.3, but also the angular distributions of W^+W^- and ZZ decay products are sensitive to the CP properties of the Higgs-boson [16]. We use the following form of a coupling to vector boson Z of a scalar (H) and a pseudoscalar (A):

$$g_{HZZ} = ig \frac{M_Z}{\cos \theta_W} (\lambda_H \cdot g^{\mu\nu}) = g_{HZZ}^{SM} \lambda_H, \quad (2)$$

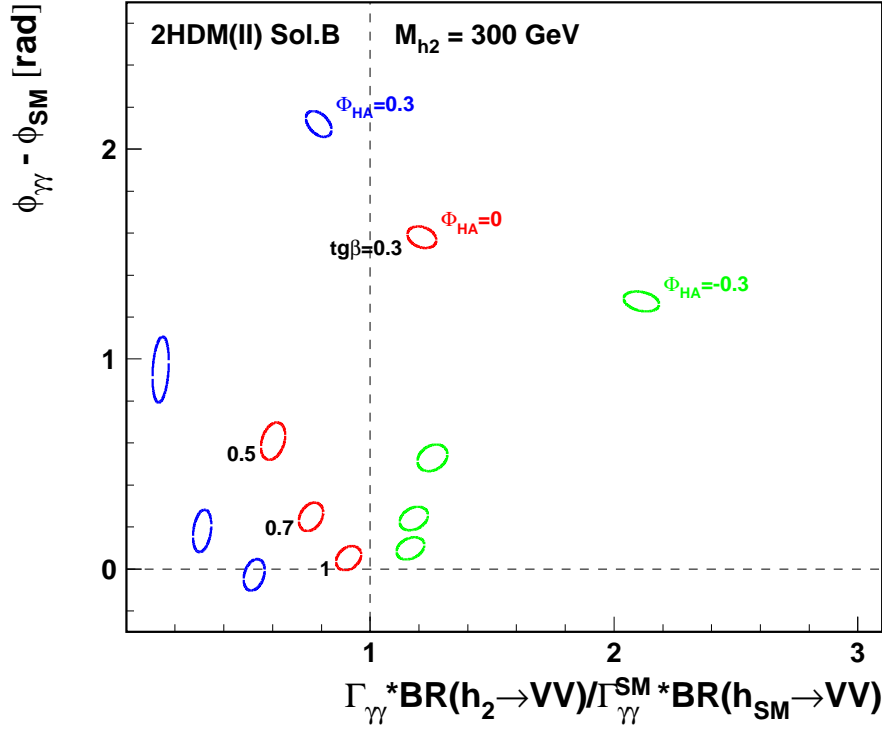


Figure 7: As in Fig.5 for the SM-like 2HDM II (B) with CP-violation for the heavy Higgs-boson h_2 with mass 300 GeV and couplings from Eq. 1. A light Higgs-boson has mass $M_{h_1} = 120$ GeV. Three values of $H - A$ mixing angle $\Phi_{HA} = -0.3, 0, 0.3$ are considered.

$$g_{AZZ} = ig \frac{M_Z}{\cos \theta_W} \left(\lambda_A \cdot \varepsilon^{\mu\nu\rho\sigma} \frac{(p_1 + p_2)_\rho (p_1 - p_2)_\sigma}{M_Z^2} \right), \quad (3)$$

where p_1 and p_2 are the 4-momenta of the vector bosons.

The coupling with λ_H corresponds to the SM-like CP-even coupling, whereas the one with λ_A is a general CP-odd coupling for the spin-0 boson (higgs). And we use similar expressions for the coupling to W , with an obvious change M_Z to M_W in the denominator of the pseudoscalar coupling, and a change in normalization factor as in the SM, namely $M_Z / \cos \theta_W \rightarrow M_W$. We see, that if $\lambda_H = 1$, the scalar H behaves as the SM Higgs boson.

3.1 Angular distributions for secondary decays

Angular variables which can be used in the analysis of CP-properties are defined in Fig. 9. To test CP-properties of the Higgs-bosons one can use the distributions of the polar angles Θ_1 and Θ_2 as well as the $\Delta\phi$ distribution, where $\Delta\phi$ is the angle between two Z - or two W - decay planes. To simplify the analysis, instead of two-dimensional distribution in $(\cos \Theta_1, \cos \Theta_2)$ we

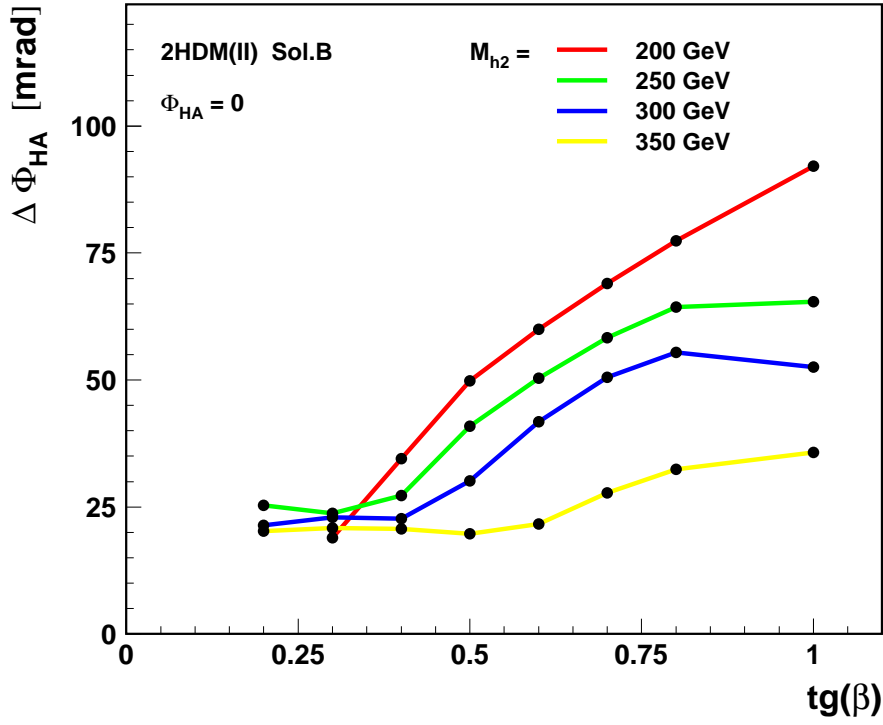


Figure 8: Verifying a CP-conservation for the SM-like 2HDM II (B). Statistical error in the determination of the $H - A$ mixing angle Φ_{HA} , as a function of $\tan\beta$ value, for four values of heavy Higgs-boson mass M_{h_2} . The simultaneous fit to the observed W^+W^- and ZZ mass spectra, with light Higgs-boson mass of 120 GeV, charged Higgs-boson mass of 800 GeV, and no $H - A$ mixing ($\Phi_{HA} = 0$), Eq. 1.

consider the distribution in a new variable, defined as

$$\zeta = \frac{\sin^2 \Theta_1 \cdot \sin^2 \Theta_2}{(1 + \cos^2 \Theta_1) \cdot (1 + \cos^2 \Theta_2)}. \quad (4)$$

The ζ -distribution corresponds to the ratio of the angular distributions expected for the decay of a scalar and a pseudoscalar (in a limit $M_h \gg M_Z$) [16].

The angular distributions in $\Delta\phi$ and ζ , expected for a scalar and a pseudoscalar higgs (Eq. 3) $h \rightarrow ZZ \rightarrow l^+l^-jj$ are compared in Fig. 10. Both distributions clearly distinguish between decays of scalar and pseudoscalar higgs. For the scalar higgs the distributions are almost flat in both $\Delta\phi$ and ζ , whereas the pseudoscalar coupling (see Eq. 3) introduces a significant $\Delta\phi$ and ζ dependence. From the measurement of these distributions we can try to establish the CP properties of the Higgs boson, even without taking into account the production mechanism. Such measurement should be considered as the most general one, as in principle some unknown heavy charged particles can significantly modify the production vertex, affecting the invariant-mass distributions on which the measurements of the two-photon width and two-photon phase are based.

Note, that the distribution of the higgs decay-angle Θ_h is expected to be flat both for scalar and pseudoscalar higgses. However, the corresponding angular distribution it is not flat for the non-resonant background. Therefore the observed Θ_h distributions, where obviously a signal, background and possible interference between them contribute, maybe be sensitive to the Higgs-boson couplings.

3.2 Generic model with CP violating couplings

Following the analysis described in [16] we consider a generic higgs model with the following tensor couplings of a Higgs boson, denoted below by \mathcal{H} , to ZZ and W^+W^- :

$$g_{\mathcal{H}ZZ} = ig \frac{M_Z}{\cos \theta_W} \left(\lambda_H \cdot g^{\mu\nu} + \lambda_A \cdot \varepsilon^{\mu\nu\rho\sigma} \frac{(p_1 + p_2)_\rho (p_1 - p_2)_\sigma}{M_Z^2} \right) \quad (5)$$

$$g_{\mathcal{H}WW} = ig M_W \left(\lambda_H \cdot g^{\mu\nu} + \lambda_A \cdot \varepsilon^{\mu\nu\rho\sigma} \frac{(p_1 + p_2)_\rho (p_1 - p_2)_\sigma}{M_W^2} \right) \quad (6)$$

The Standard Model couplings are reproduced for $\lambda_H = 1$ and $\lambda_A = 0$. Below we will

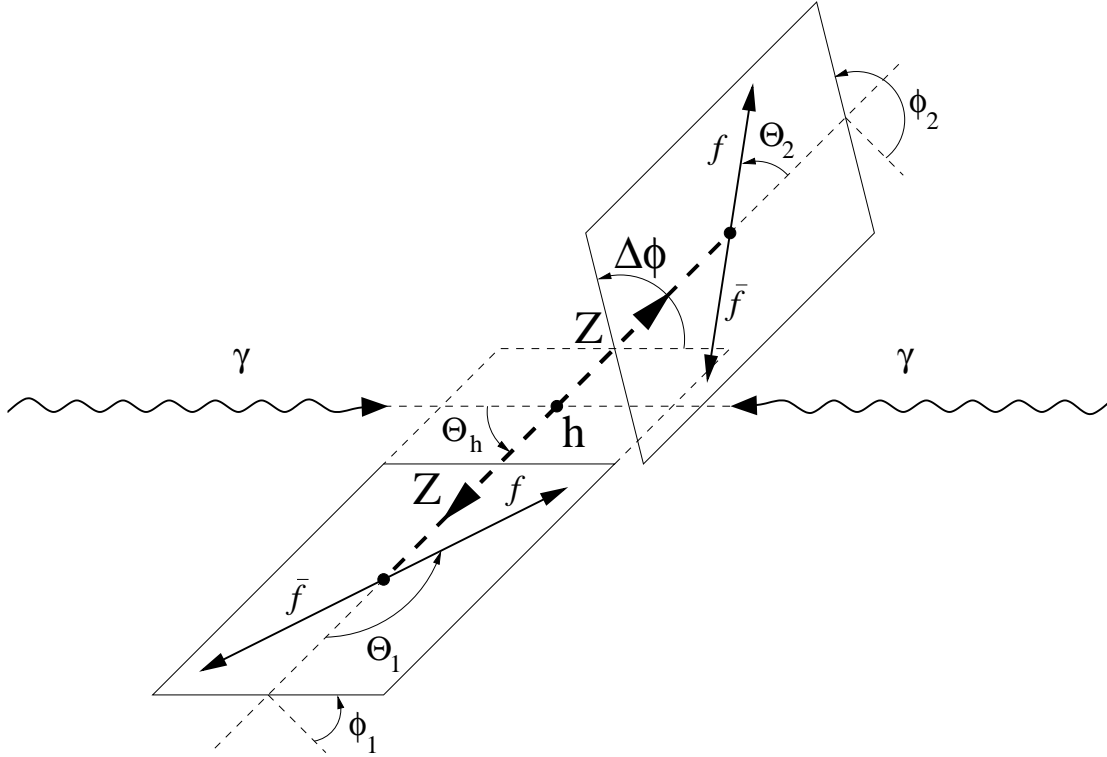


Figure 9: The definition of the polar angles Θ_h , Θ_1 and Θ_2 , and the azimuthal angles ϕ_1 and ϕ_2 for the process $\gamma\gamma \rightarrow h \rightarrow ZZ \rightarrow 4 f$. $\Delta\phi$ is the angle between two Z decay planes, $\Delta\phi = \phi_2 - \phi_1$. All polar angles are calculated in the rest frame of the decaying particle.

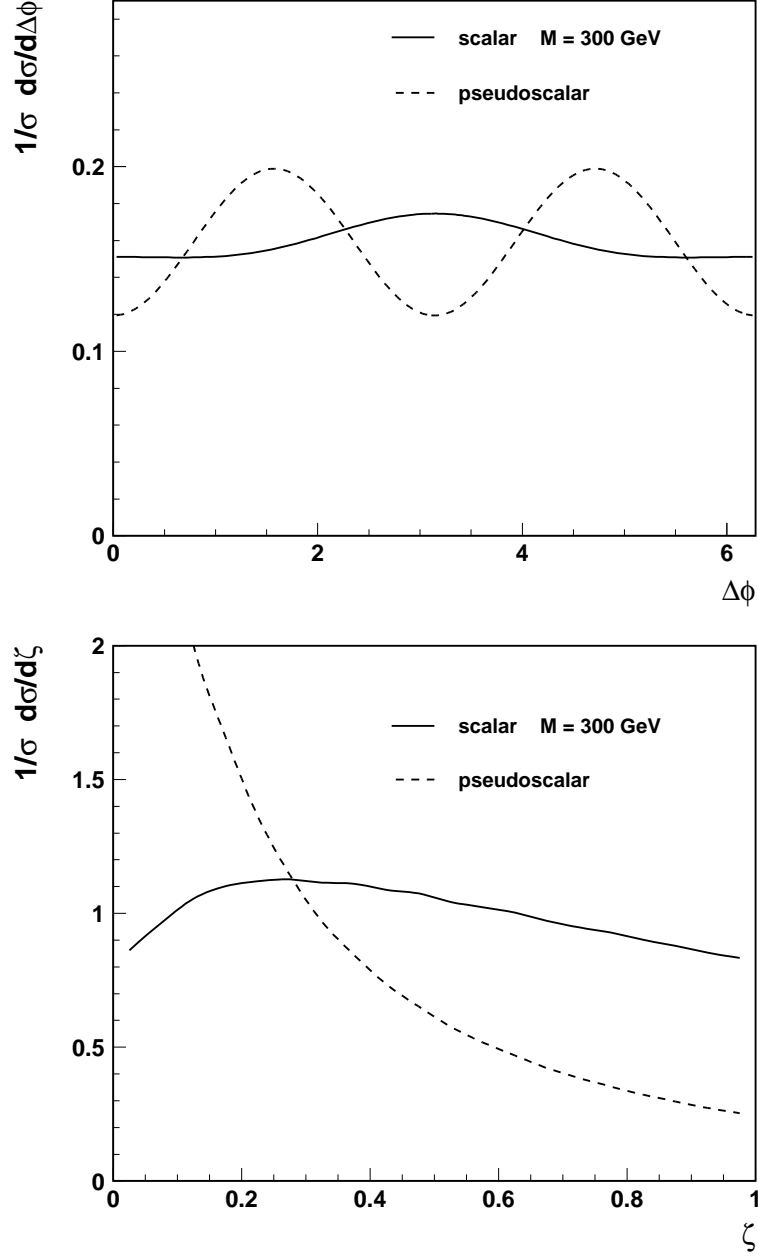


Figure 10: Normalized angular distributions in $\Delta\phi$ (upper plot) and ζ (lower plot), expected (Eq. 3) for scalar and pseudoscalar higgs decays $H, A \rightarrow ZZ \rightarrow l^+l^-jj$, for the higgs mass of 300 GeV.

consider only small deviations from the Standard Model, i.e. $\lambda_H \sim 1$ and $|\lambda_A| \ll 1$. To simplify the case, we assume that higgs \mathcal{H} couplings to fermions are the same as in the Standard Model.

3.3 Reconstruction of the angular distributions

Measurement of the angular distributions has been studied using samples of ZZ events generated with PYTHIA and SIMDET programs, as described in section 2.1. The resolutions of the reconstructed decay angles Θ and ϕ , for leptonic and hadronic Z decays, are compared in Fig. 11, for the scalar Higgs-boson with mass of 300 GeV.

A very good resolution is obtained for all considered distributions, nevertheless the measured angular distributions are strongly affected by the selection cuts used in the analysis. Because of the cut on the lepton and jet angles, applied to preserve a good mass resolution (see [2] for more details), we observe significant loss of the selection efficiency for events with lepton or jet emitted along the beam direction. Also the Durham jet algorithm used in the event reconstruction imposes constraints on the angular separation between leptons and jets. Both effects result in a highly non-uniform angular acceptance. Selection efficiencies for $\gamma\gamma \rightarrow ZZ \rightarrow l^+l^-jj$ events, as a function of the angle $\Delta\phi$, are presented in Fig. 12. We consider reconstructed $\Delta\phi$ values from 0 to π , since we are not able to distinguish between quark and antiquark jet. The efficiencies for ZZ events coming from decays of scalar, pseudoscalar higgs and non-resonant background are compared. The polar-angle distributions differ among these three classes of events, what leads to a significantly different acceptances. This simulation was performed for primary electron-beam energy of 209 GeV optimal for a Higgs-boson mass of 300 GeV. An additional cut on the reconstructed ZZ invariant-mass has been introduced to optimise the signal measurement from the angular distribution. We found that for higgs mass of 300 GeV the accepted mass range lies between 286 and 312 GeV. This cuts affects mainly the non-resonant background events.

We calculate the expected angular distributions for ZZ and W^+W^- events by convoluting the corresponding cross-section formula with the CompAZ photon-energy spectra, and in addition with the parametrization of the invariant-mass resolution and acceptance function including the angular- and jet-selection cuts. Here we neglect (small) effects of the angular resolution. For the measurement of the event distributions in $\Delta\phi$ and ζ we introduce the additional cuts on the reconstructed ZZ invariant mass (for ZZ events) or on the reconstructed W^+W^- invariant mass as well as the higgs-decay angle Θ_h (for W^+W^- events). The cuts were optimised for the smallest relative error in the signal cross-section measurement.

Expected precision in the measurements of the angle $\Delta\phi$ and of the variable ζ distributions, for $\gamma\gamma \rightarrow ZZ \rightarrow l^+l^-jj$ events and $\gamma\gamma \rightarrow W^+W^- \rightarrow 4j$ events are illustrated in Figs. 13 and 14, respectively. Calculations were performed for primary electron-beam energy of 209 GeV and the Higgs-boson mass of 300 GeV. The results, presented relative to the SM prediction, are confronted in Figs. 13 (14) with the expectations of the generic model with $\lambda_A = \pm 0.2$ and $\lambda_H = 1$ ($\lambda_A = 0.2$ and $\lambda_H = 1$; $\lambda_A = 0$ and $\lambda_H = 1.1$), for the reconstructed ZZ (W^+W^-) events. We see, that the generic model predicts deviations both in the normalization and in the shape of angular distributions. Therefor we should be able to constrain Higgs-boson couplings

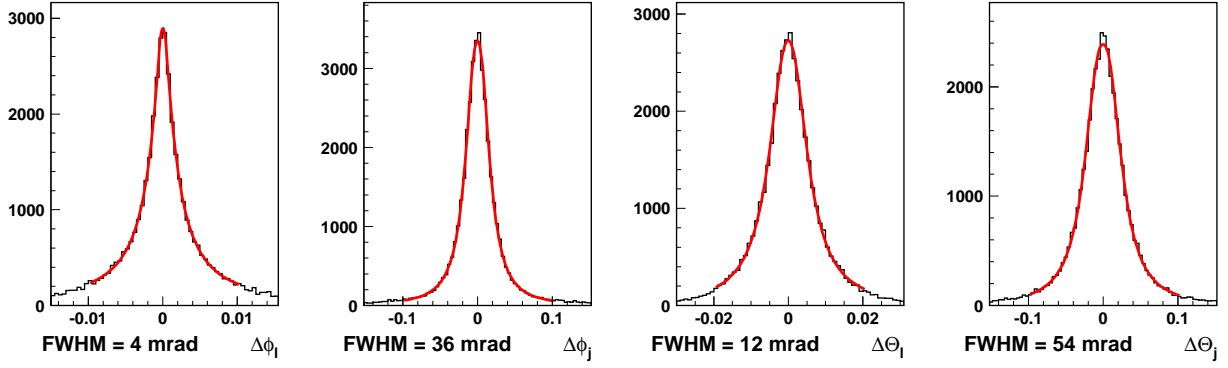


Figure 11: Resolution in the reconstructed Z -decay angles Θ and ϕ , for the leptonic (Θ_l , ϕ_l) and hadronic (Θ_j , ϕ_j) final states. Events were simulated with the PYTHIA and SIMDET programs, for a primary electron-beam energy of 209 GeV and scalar Higgs-boson mass of 300 GeV.

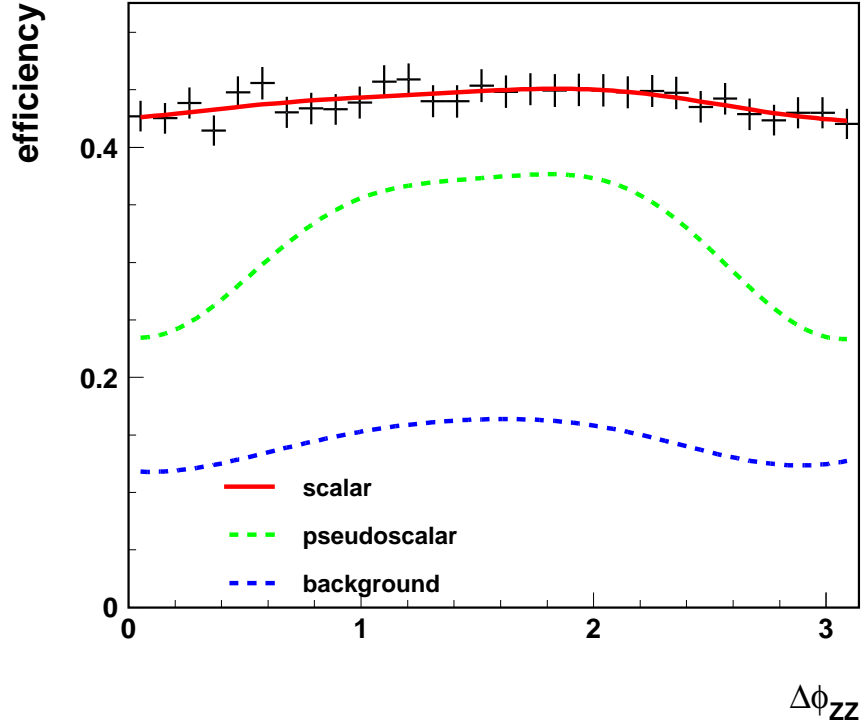


Figure 12: Selection efficiency as a function of the angle $\Delta\phi$ between two Z decay planes, for $ZZ \rightarrow l^+l^-jj$ events coming from the scalar higgs decays, pseudoscalar higgs decays and non-resonant background. Events were simulated with the PYTHIA and SIMDET programs, for a primary electron-beam energy of 209 GeV and Higgs-boson mass of 300 GeV. Only events with the reconstructed higgs mass between 286 and 312 GeV are accepted.

from the shape of the distributions, even if the overall normalization related to the Higgs-boson production mechanism is not known.

3.4 Determination of CP properties of the Higgs boson from the measurement of angular distributions

Each of the considered angular distributions discussed above can be fitted with a model expectations, given in terms of the parameters λ_A and λ_H . If we do not use normalisation constraints (i.e. do not assume a given production mechanism) there are large correlations between λ_A and λ_H in fits to a single-variable distributions, i.e. for $\Delta\phi$, ζ and Θ_h . Therefore we first limit ourselves to $\lambda_H = 1$ case. Statistical errors in the determination of λ_A from the fits to the shape of various angular distributions, to be obtained after one year of photon collider running, are presented in Fig. 15, separately for the WW and ZZ channels. In the figure we present also the results obtained from the simultaneous (combined) fit to all three considered distributions. It turns out that both for ZZ and for W^+W^- events the measurement of the ζ -distribution gives the best constraints on the λ_A parameter, and a precision of λ_A measurement from the ζ distribution only is close to the precision obtained from the combined fit. For $M_h \geq 250$ GeV the expected accuracy for λ_A is about 0.1 both for the ZZ and for W^+W^- events.

Finally we estimate the expected statistical errors from the combined fit to angular distributions of ZZ and W^+W^- events, they are shown in Fig. 16. By fitting all angular distributions simultaneously we found the error on λ_A of 0.06–0.08 for $M_h \geq 200$ GeV.

In case of the combined fit, correlations between λ_A and λ_H parameters are smaller, so both parameters can be fitted simultaneously. Expected statistical errors on λ_A and λ_H are shown in Fig. 17. For low Higgs-boson masses, $M_h \leq 250$ GeV, better constraints are obtained from the measurement of W^+W^- events, whereas for $M_h \geq 300$ GeV smaller errors are obtained from the measurement of ZZ events. Expected error on λ_A is below 0.1 for $M_h \leq 200$ GeV, while the corresponding error on λ_H changes from about 0.1 to 0.3 with increasing Higgs-boson mass.

3.5 Determination of CP properties from the combined analysis of the invariant-mass and angular distributions

Significantly better constraints on the model parameters λ_A and λ_H can be obtained if we assume that there is no “new physics” except for the considered anomalous couplings of the Higgs-boson to W^+W^- and ZZ . We can then calculate the expected invariant-mass distributions for ZZ and W^+W^- events. In Fig. 18 and 19 statistical errors on the measured invariant-mass distributions, expected after one year of photon collider running at a nominal luminosity, are compared with the predictions of the generic model. We see, that large deviations from the Standard Model prediction are expected for $\lambda_A \neq 0$, mainly due to the interference effects.

Expected statistical errors in the determination of λ_A and λ_H from the combined fit to

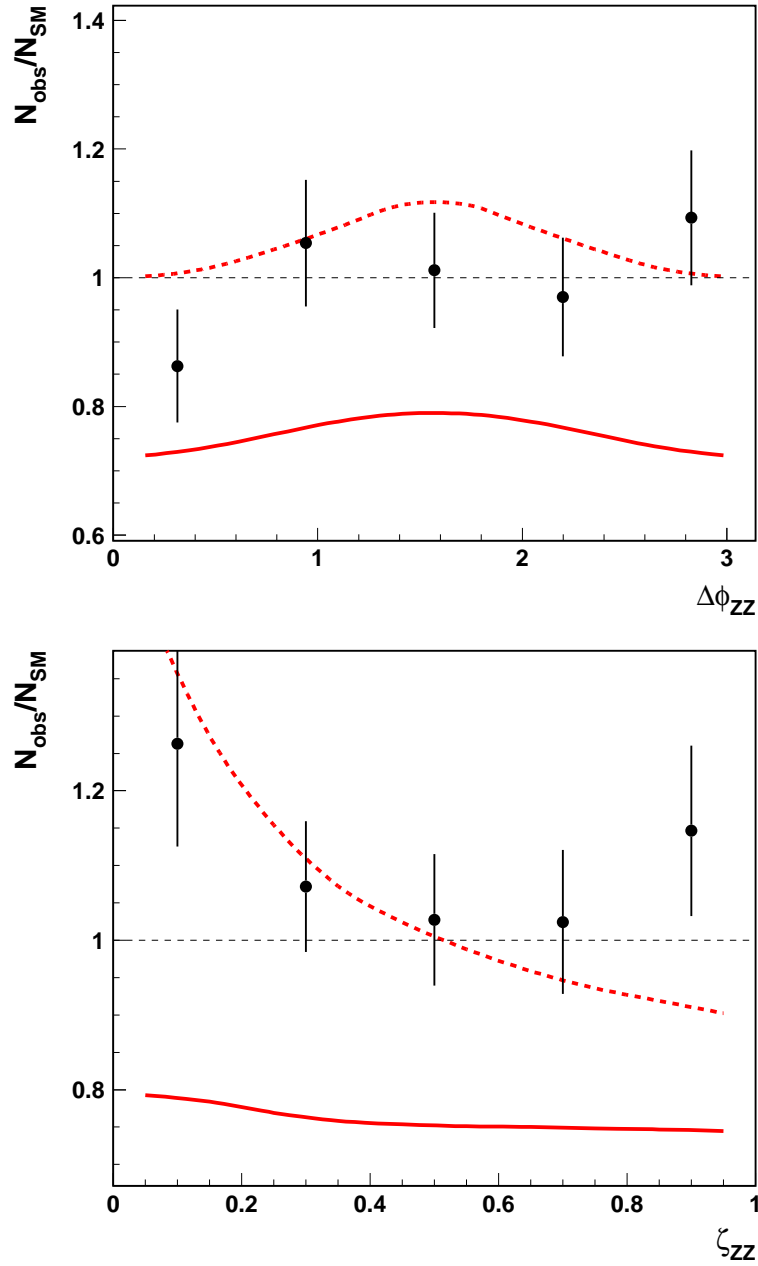


Figure 13: Expected deviations from the Standard Model predictions for $ZZ \rightarrow l^+l^-jj$ events, for the measurement of the angle $\Delta\phi_{ZZ}$ between two Z -decay planes (upper plot) and of the variable ζ_{ZZ} calculated from the polar angles of the $Z \rightarrow l^+l^-$ and $Z \rightarrow jj$ decays (lower plot). Solid (dashed) red line correspond to the model with $\lambda_H = 1$ and $\lambda_A = 0.2$ ($\lambda_A = -0.2$). Signal and background calculations are performed for primary electron-beam energy of 209 GeV and the Higgs-boson mass of 300 GeV. Only events with reconstructed higgs mass between 286 and 312 GeV are accepted.

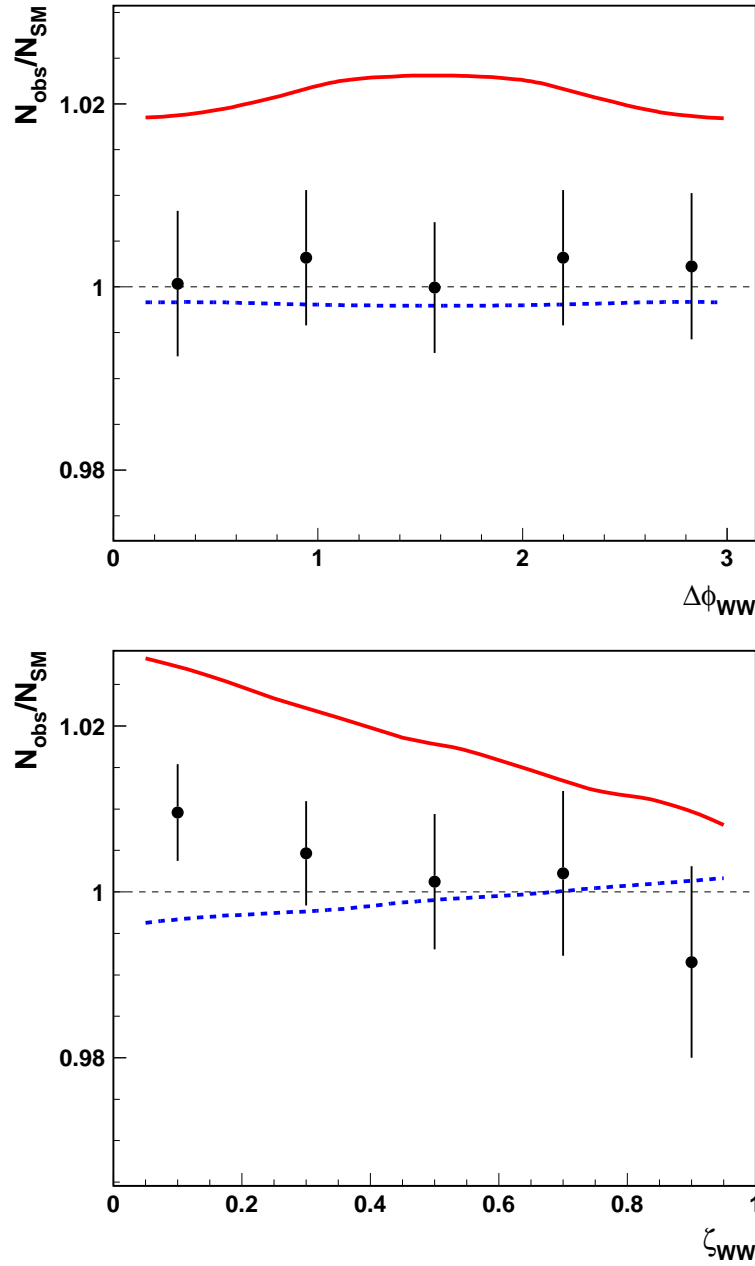


Figure 14: Expected deviations from the Standard Model predictions for $W^+W^- \rightarrow 4j$ events, for the measurement of the angle $\Delta\phi_{WW}$ between two W -decay planes (upper plot) and of the variable ζ_{WW} calculated from the polar angles of two $W \rightarrow jj$ decays (lower plot). Solid red (dashed blue) line correspond to the model with $\lambda_A = 0.2$ and $\lambda_H = 1$ ($\lambda_A = 0$ and $\lambda_H = 1.1$). Signal and background calculations are performed for primary electron-beam energy of 209 GeV and the Higgs-boson mass of 300 GeV. Correlated cuts on the reconstructed mass and higgs decay angle were imposed to improve signal to background ratio.

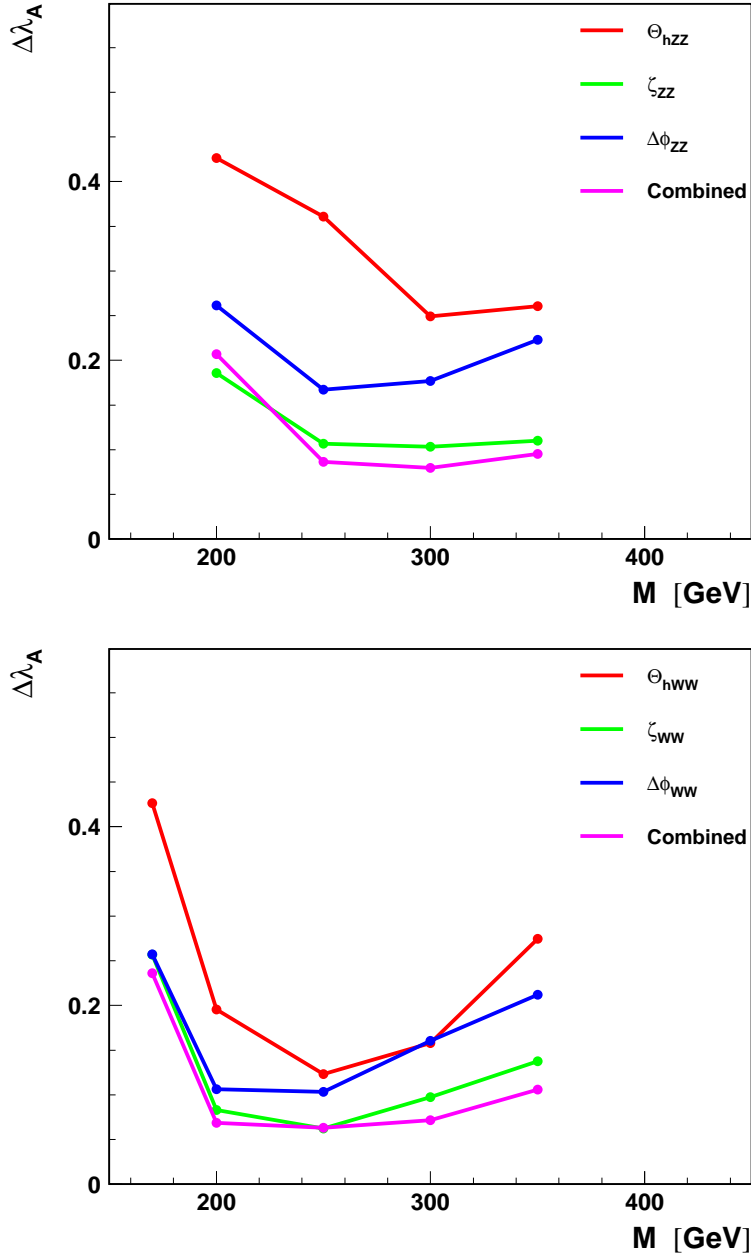


Figure 15: Statistical error in the determination of λ_A , expected after one year of photon collider running, as a function of the Higgs-boson mass M . Fits were performed to the shape of three individual angular distributions, as indicated in the plots, separately for ZZ events (upper plot) and W^+W^- events (lower plot). Results of the simultaneous fits to all three considered distributions are also given. Parameter λ_H is fixed to the Standard Model value, $\lambda_H = 1$. No normalisation constraints are imposed. Errors resulting from the fit were calculated for $\lambda_A = 0$.

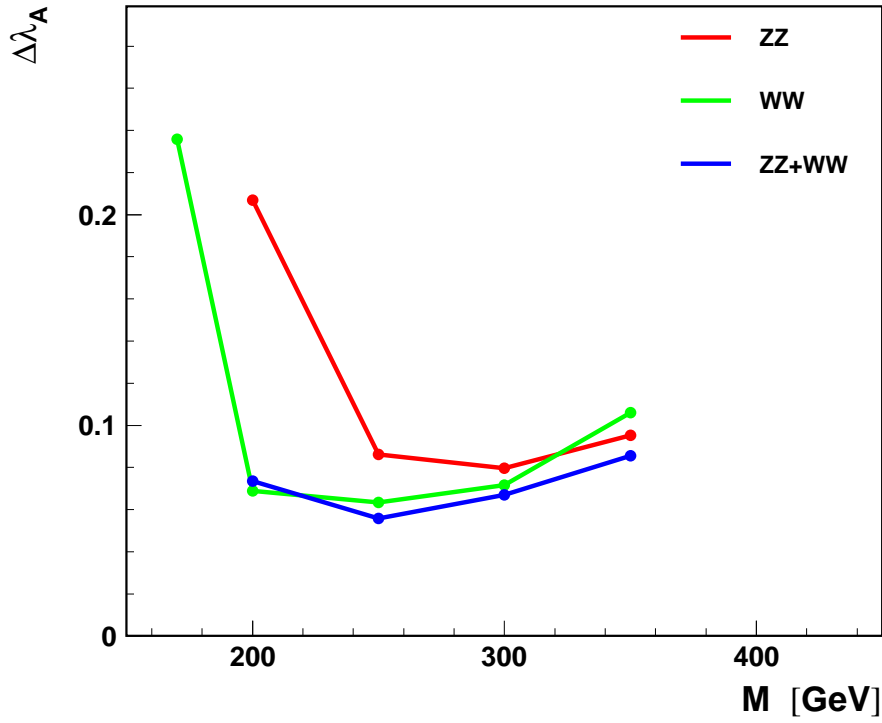


Figure 16: Statistical error in the determination of λ_A , expected after one year of photon collider running, as a function of the Higgs-boson mass M . Results from the simultaneous fits to all considered angular distributions for ZZ and W^+W^- events, and from the combined fit for both ZZ and W^+W^- events are compared. Parameter λ_H is fixed to the Standard Model value, $\lambda_H = 1$. No normalisation constraints are imposed. Errors resulting from the fit were calculated for $\lambda_A = 0$.

angular distributions and invariant-mass distributions are compared in Fig. 20. A relative normalisation of ZZ and W^+W^- samples is imposed in the fit, as predicted from the cross section calculations. However, overall normalisation, corresponding to the integrated luminosity of the considered data sample, is allowed to vary. For $M_h \geq 200$ GeV the error on λ_A of about 0.01 can be achieved from the combined fit to all considered distributions. The value of λ_A is mainly constrained by the measurement of the invariant-mass distribution for W^+W^- events. Expected statistical error on λ_H is slightly bigger, between 0.01 and 0.02, and comes mainly from the measurement of the invariant-mass distribution for ZZ events.

4 Summary

An opportunity of measuring of the Higgs-boson properties at the the Photon Collider at TESLA has been studied in detail for masses between 180 and 350 GeV, using realistic lu-

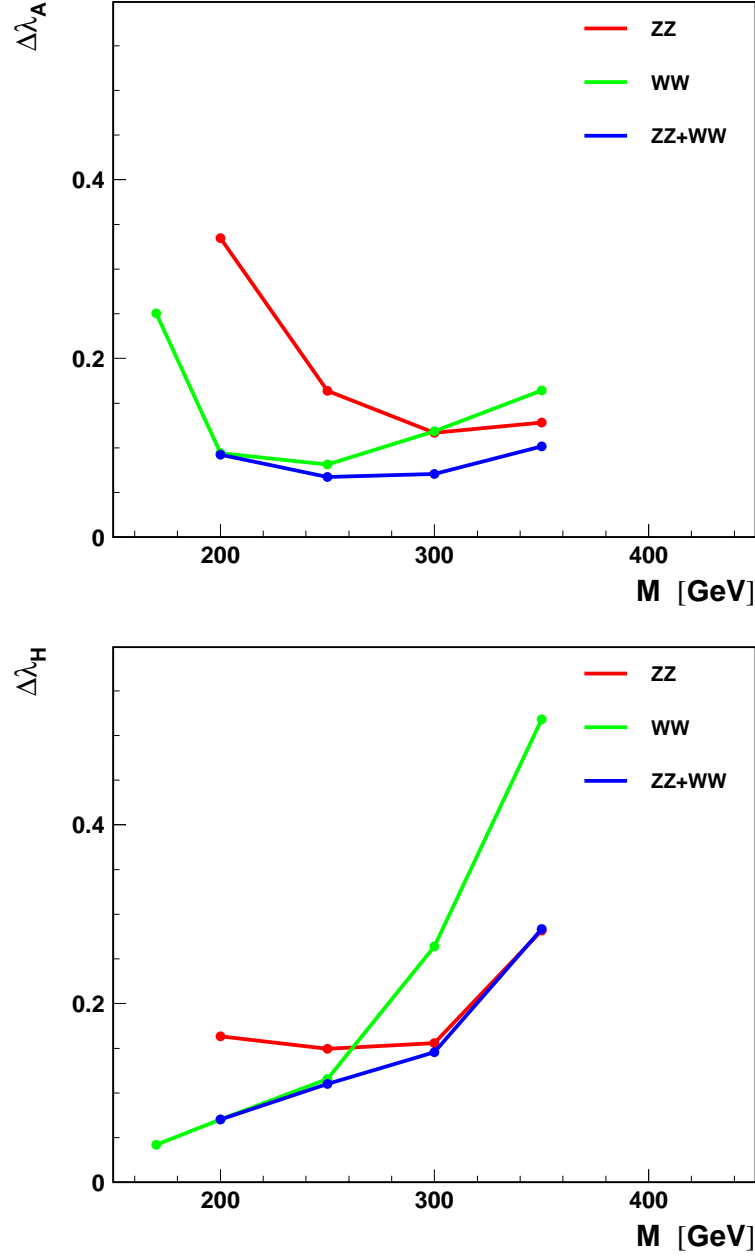


Figure 17: As in 16, for λ_A (upper plot) and λ_H (lower plot), for determination of both parameters from simultaneous fit to all considered angular distributions.

minosity spectra and detector simulation. We found that from the combined measurement of the invariant-mass distributions in the ZZ and W^+W^- decay-channels, the parameters of the SM-like Two Higgs Doublet Model can be precisely determined. For both light and heavy scalar Higgs boson, a statistical precision in the determination of its coupling ($\tan\beta$) is of the order of 10% already after one year of Photon Collider running. In case of the Two Higgs Doublet Model with a CP violation, the $H - A$ mixing angle can be determined with statistical precision of 20 to 90 mrad (in a small-mixing approximation).

We also considered the combined measurement of the various angular correlations in the W^+W^- and ZZ -decay products. For a simple generic model, with SM-couplings to fermions, the parameters describing a CP violation in the higgs couplings to vector bosons can be determined to about 10%. If in addition the invariant-mass distribution is used to constrain model parameters, 1–2 % statistical uncertainty in the determination of the Higgs-boson couplings can be achieved.

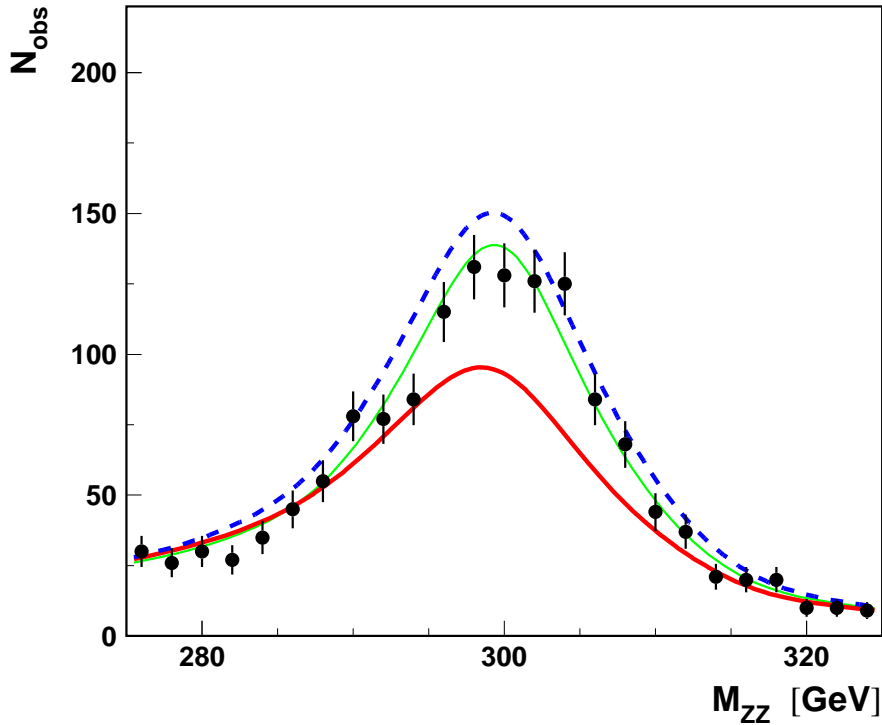


Figure 18: Predictions for the measurement of the ZZ invariant mass M_{ZZ} , for $ZZ \rightarrow l^+l^-jj$ events. Solid red (dashed blue) line correspond to the generic model with $\lambda_A = 0.2$ and $\lambda_H = 1$ ($\lambda_A = 0$ and $\lambda_H = 1.1$). Thin green line corresponds to the Standard Model predictions ($\lambda_A = 0$ and $\lambda_H = 1$). Points with error bars indicate the statistical precision of the measurement after one year of photon collider running at nominal luminosity. Signal and background calculations are performed for primary electron-beam energy of 209 GeV optimal for the Higgs-boson mass of 300 GeV.

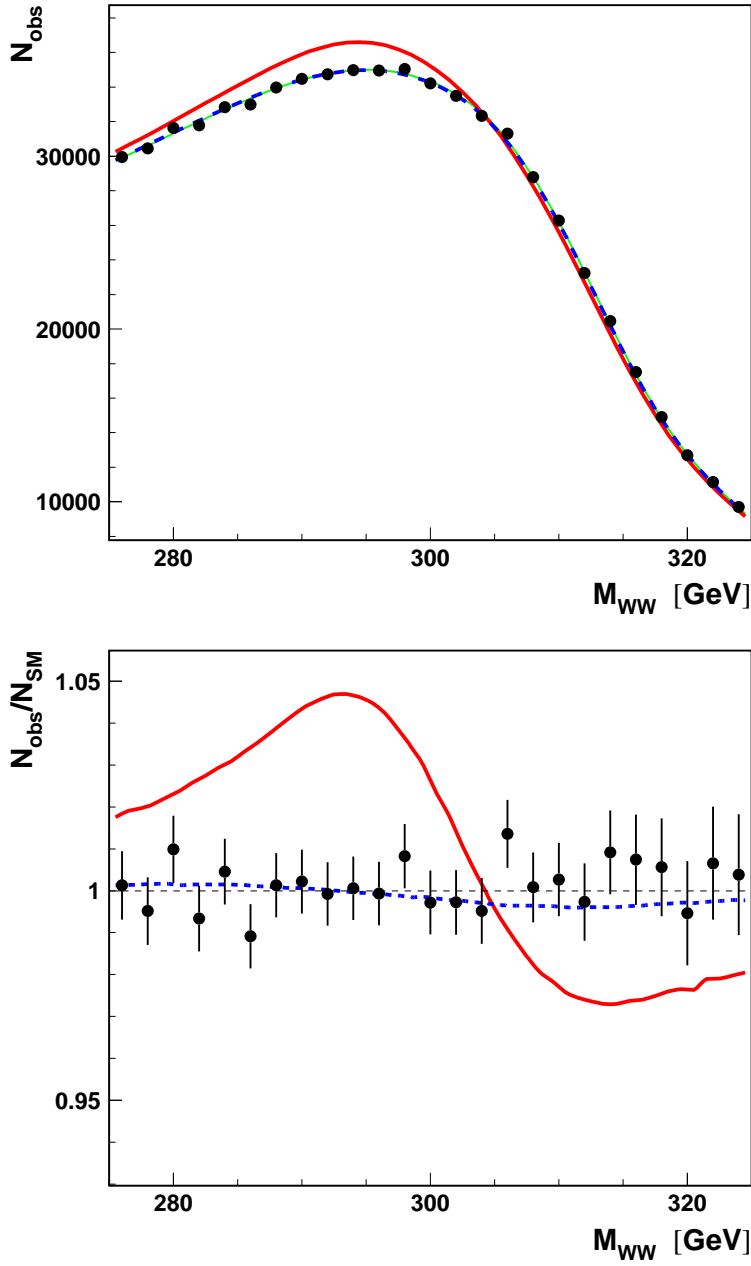


Figure 19: Expected deviations from the Standard Model predictions for the measurement of the W^+W^- invariant mass M_{WW} , for $W^+W^- \rightarrow 4j$ events. Invariant-mass distribution measured after one year of photon collider running at nominal luminosity (upper plot) and the ratio of this distribution to the SM predictions (lower plot) are shown. Solid red (dashed blue) line correspond to the model with $\lambda_A = 0.2$ and $\lambda_H = 1$ ($\lambda_A = 0$ and $\lambda_H = 1.1$). Thin green line (upper plot) corresponds to the Standard Model predictions ($\lambda_A = 0$ and $\lambda_H = 1$). Signal and background calculations are performed for primary electron-beam energy of 209 GeV optimal the Higgs-boson mass of 300 GeV.

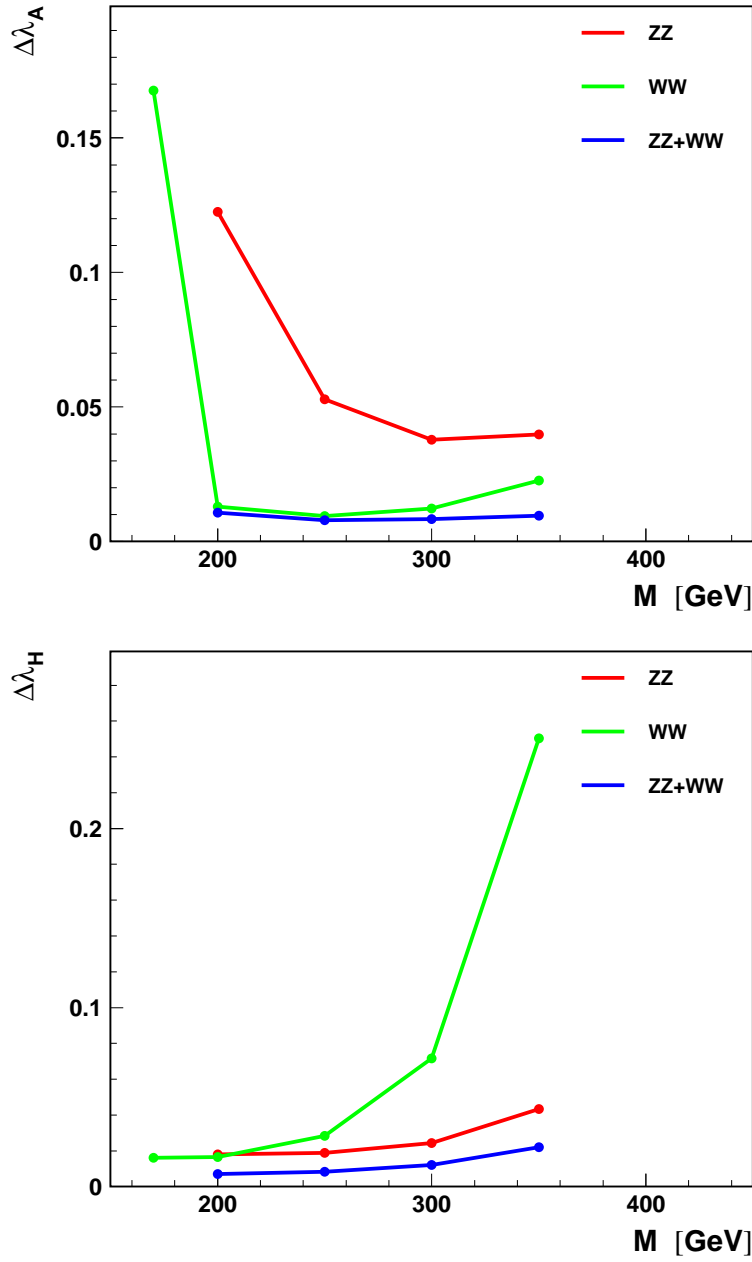


Figure 20: Statistical error in the determination of λ_A (upper plot) and λ_H (lower plot), expected after one year of photon collider running, as a function of the Higgs-boson mass M . Results from the simultaneous fits to all considered angular distributions and invariant-mass distributions for ZZ and W^+W^- events, and from the combined fit for both ZZ and W^+W^- events are compared. Relative normalisation of ZZ and W^+W^- samples is imposed in the fit. Errors resulting from the simultaneous fit of both parameters were calculated for $\lambda_A = 0$ and $\lambda_H = 1$.

Acknowledgements

We are especially grateful to David Miller for stimulating discussions. We would also like to thank other colleagues from the ECFA/DESY Study for useful comments and suggestions. M.K. acknowledges partial support by Polish Committee for Scientific Research, Grant 5 P03B 121 20 (2003), and by the European Community's Human Potential Programme under contract HPRN-CT-2000-00149 Physics at Colliders.

References

- [1] B. Badelek et al., *Photon Collider at TESLA*, TESLA Technical Design Report, Part 6, Chapter 1, DESY-2001-011, ECFA-2001-209, DESY-TESLA-2001-23, DESY-TESLA-FEL-2001-05, March 2001, hep-ex/0108012.
- [2] P.Nieżurawski, A.F.Żarnecki, M.Krawczyk, JHEP 0211 (2002) 034 [hep-ph/0207294]
- [3] I. F. Ginzburg and I. P. Ivanov, *Phys. Lett.* B408 (1997) 325.
- [4] G.J. Gounaris, J. Layssac, P.I. Porfyriadis, F.M. Renard, *Eur.Phys.J.* C13 (2000) 79.
- [5] G.J. Gounaris, P.I. Porfyriadis and F.M. Renard, *Eur. Phys. J.* C19 (2001) 57.
- [6] E. Asakawa, J. i. Kamoshita, A. Sugamoto and I. Watanabe, *Eur. Phys. J.* C14 (2000) 335; E. Asakawa, S. Y. Choi, K. Hagiwara and J. S. Lee, *Phys. Rev.* D62 (2000) 115005.
- [7] E. Asakawa and K. Hagiwara, hep-ph/0305323.
- [8] I. F. Ginzburg, G. L. Kotkin, V. G. Serbo and V. I. Telnov, *Pizma ZhETF* 34, 514 (1981), *JETP Lett.* 34, 491 (1982); Preprint INP 81-50, Novosibirsk, 1981 and *Nucl. Instrum. Meth. A* 205, 47 (1983); Preprint INP 81-102, Novosibirsk, 1981;
I. F. Ginzburg, G. L. Kotkin, S. L. Panfil, V. G. Serbo and V. I. Telnov, *Nucl. Instrum. Meth. A*219, 5 (1984);
V. I. Telnov, *Nucl. Instrum. Meth. A*294, 72 (1990).
- [9] A.F. Żarnecki, *Acta Phys.Polon.* B34 (2003) 2741 [hep-ex/0207021],
<http://info.fuw.edu.pl/~zarnecki/compaz/compaz.html>
- [10] V. I. Telnov *Nucl. Instrum. Meth. A* 355 (1995) 3; V. I. Telnov, *A Code for the simulation of luminosities and QED backgrounds at photon colliders*, talk presented at Second Workshop of ECFA-DESY study, Saint Malo, France, April 2002.
- [11] G.Belanger, F.Boudjema, *Phys. Lett.* B288 (1992) 210; D.A.Morris, et al., *Phys. Lett.* B323 (1994) 421.
- [12] T. Sjostrand, P. Eden, C. Friberg, L. Lonnblad, G. Miu, S. Mrenna and E. Norrbin, *Comp. Phys. Comm.* 135 (2001) 238.

- [13] M. Pohl, H. J. Schreiber, DESY-99-030.
- [14] I. F. Ginzburg, M. Krawczyk and P. Osland, *Nucl. Instrum. Meth.* A472:149, 2001 [hep-ph/0101229]; hep-ph/0101331; hep-ph/0101208.
- [15] I. F. Ginzburg, M. Krawczyk and P. Osland, *Two-Higgs-doublet models with CP violation*, presented at International Workshop on Linear Colliders (LCWS 2002), Jeju Island, Korea, August 2002, hep-ph/0211371.
- [16] D.J. Miller, S.Y. Choi, B. Eberle, M.M. Mühlleitner and P.M. Zerwas, *Phys. Lett.* B505 (2001) 149 [hep-ph/0102023]; S.Y. Choi, D.J. Miller, M.M. Mühlleitner and P.M. Zerwas, hep-ph/0210077; D.J. Miller, *Spin and Parity in the HZZ vertex*, presented at the ECFA/DESY meeting, Prague, November 2002.